

# Study of Beta Equilibrated 2+1 Flavor Quark Matter in PNJL Model

Abhijit Bhattacharyya\*

*Department of Physics, University of Calcutta, 92, A.P.C Road, Kolkata-700009, India*

Sanjay K Ghosh,<sup>†</sup> Sarbani Majumder,<sup>‡</sup> and Rajarshi Ray<sup>§</sup>

*Center for Astroparticle Physics & Space Science,  
Block-EN, Sector-V, Salt Lake, Kolkata-700091, INDIA*

*Department of Physics, Bose Institute,  
93/1, A. P. C Road, Kolkata - 700009, INDIA*

We report a first case study of the phase diagram of 2+1 flavor strongly interacting matter in  $\beta$ -equilibrium, using the Polyakov–Nambu–Jona-Lasinio model. Physical characteristics of relevant thermodynamic observables have been discussed. A comparative analysis with the corresponding observables in the Nambu–Jona-Lasinio model is presented. We find distinct differences between the models in terms of a number of thermodynamic quantities like the speed of sound, specific heat, various number densities as well as entropy. The present study is expected to give us a better insight into the role that the superdense matter created in heavy ion collision experiments play in our understanding of the properties of matter inside the core of supermassive stars in the Universe.

PACS numbers: 25.75.Nq, 21.65.Qr, 26.60.Kp

## I. INTRODUCTION

The phase diagram of strongly interacting matter has been at the center of attention for quite some time now. Under a variety of extreme conditions of temperature and/or density the hadrons may overlap and lose their individuality and a new state of matter called Quark Gluon Plasma (QGP) may be formed [1]. It is well believed that such a state of matter existed in the hot early Universe, a few microseconds after the Big Bang. Deconfined quark matter could also exist in the core of neutron stars (NS) [2–4] where the temperature is relatively low but density is high. So an understanding of the physics of strongly interacting matter at such environmental conditions would have important cosmological and astrophysical significance.

In the laboratory such conditions of large temperatures and densities can be created by the collision of heavy ions at high energies. Presently the strongly interacting matter at high temperature and close to zero baryon densities – a scenario relevant for early universe – is being explored at Relativistic Heavy Ion Collider (RHIC) at BNL and the Large Hadron Collider (LHC) at CERN. A wealth of information has been obtained from RHIC, and a lot more is expected from both the future runs there as well as from LHC. More recently a variety of energy scans at RHIC and the upcoming facility (FAIR) at GSI, are expected to give us a glimpse of matter in the baryon-rich environments – the so-called *compressed baryonic matter* (CBM). These experiments will also be useful in the search for signatures of critical phenomena associated with a second order critical end point (CEP).

At the same time, observational data are being collected by a large number of telescopes and satellites [5] such as the radio telescopes at the Arecibo, Parkes, Jodrell Bank, and Green Bank Observatories, the Hubble Space Telescope, European Space Agency’s International Gamma Ray Astrophysics Laboratory (INTEGRAL) satellite, Very Large Telescope (VLT) of the European Southern Observatory, the X-ray satellites Chandra, XMM-Newton and NASA’s Rossi X-ray Timing Explorer and the Swift satellite. Observations from these facilities are supposed to tell us about the properties of strongly interacting matter at high densities relevant for the astrophysics of compact stars.

Thus on one hand the laboratory experiments are expected to scan the phase space temperature and various conserved quantum number densities of strongly interacting matter. On the other hand the astrophysical observations are expected to uncover the physics for high baryon number density region of the phase diagram. It should be noted here that the physical characteristics of the matter under consideration may be quite different in the two cases.

---

\*Electronic address: abphy@caluniv.ac.in

†Electronic address: sanjay@bosemain.boseinst.ac.in

‡Electronic address: sarbanimajumder@gmail.com

§Electronic address: rajarshi@bosemain.boseinst.ac.in

The time-scale of the dynamics of heavy-ion experiments is so small that only strong interactions may equilibrate thermodynamically. While the dynamics in the astrophysical scenario is slow enough to allow even weak interactions may equilibrate. Thus a question naturally arises – to what extent can laboratory experiments be used to infer about the compact star interiors? The aim of this paper is to address this question at a preliminary level from the characteristics of the " $\beta$ -equilibrated" phase diagrams.

One should be able to study the properties of systems described above from first principles using Quantum Chromodynamics (QCD), which is *the* theory of strong interactions. However, QCD is highly non-perturbative in the region of temperature and density that we are interested in. The most reliable way to analyze the physics in this region of interest is to perform a numerical computation of the lattice version of QCD (Lattice QCD). The scheme is robust but numerically costly. Moreover, there are problems in applying this scheme for the systems having finite baryon density. Thus it has become a common practice to study the physics of strongly interacting matter under the given conditions using various QCD inspired effective models.

Until now various quark models, such as, different versions of the MIT bag model [6, 7], the color-dielectric model [8, 9] and different formulations of the NJL model [10, 11] have been used to study the NS structure. Despite the similarity of the results on the value of the maximum NS mass, the predictions on the NS configurations can differ substantially from model to model. The most striking difference is in the quark matter content of the NS, which can be extremely large in the case of EOS related to the MIT bag model or the color-dielectric model, but it is vanishingly small in the case of the original version of the NJL model [10, 12]. In the case of NJL model it turns out that, as soon as quark matter appears at increasing NS mass, the star becomes unstable, with only the possibility of a small central region with a mixed phase of nucleonic and quark matter. This may be a result of the lack of confinement in NJL model. In fact an indirect relationship between confinement and NS stability has been found in a study using NJL model with density dependent cut-off [13]. Hence it is important to study the EOS from the Polyakov–Nambu–Jona-Lasinio (PNJL) model [14–16], where a better description of confinement has been incorporated through Polyakov loop mechanism. Moreover, a comparison with NJL model might be helpful in understanding the role of Polyakov loop at high chemical potential.

A detailed study of 2+1 flavor strong interactions have been done by some of us using the PNJL model. The general thermodynamic properties along with the phase diagram [17], as well as details of fluctuation and correlations of various conserved charges [18] have been reported. Here we extend the work by including  $\beta$ -equilibrium into the picture. In the context of NJL model such a study was done earlier in [19, 20]. The properties of pseudoscalar and neutral mesons have been studied in finite density region within the framework of 2+1 flavor NJL model in  $\beta$ -equilibrium [21, 22].

We investigate and compare different properties of the NJL and PNJL models in the  $T$ - $\mu_B$  plane. The specialization of these studies to the possible dynamical evolution of NS and/or CBM created in heavy-ion collisions will be kept as a future excersize.

The paper is organized as follows. In section II we discuss our model. In section III we calculate different thermodynamic properties and present our result and finally we conclude in section IV.

## II. FORMALISM

The supermassive compact objects like neutron stars are born in the aftermath of supernova explosions. The initial temperature of a new born NS can be as high as  $T \sim 100$  MeV. For about one minute following its birth, the star stays in a special proto-neutron star state: hot, opaque to neutrinos, and larger than an ordinary NS (see, e.g., [23, 24] and references therein). Later the star becomes transparent to neutrinos generated in its interior. It cools down gradually, initially through neutrino emission ( $t \leq 10^5$  years) and then through the emission of photons ( $t \geq 10^5$  years) [25], and transforms into an ordinary NS. The weak interaction responsible for the emission of these neutrinos eventually drive the stars to the state of  $\beta$ -equilibrium along with the imposed condition of charge neutrality.

The mass, radius and other characteristics of such a star depend on the equation of state (EOS), which in turn, is determined by the composition of the star [26]. The possible central density of a compact star may be high enough for the usual neutron-proton matter to undergo a phase transition to some exotic forms of strongly interacting matter. Some of the suggested exotic forms of strongly interacting matter are the hyperonic matter, the quark matter, the superconducting quark matter etc. If there is a hadron to quark phase transition inside the NS, then all the characteristics of the NS will depend on the nature of the phase transition [27, 28].

Furthermore, there have been suggestions that the strange quark matter, containing almost equal numbers of u, d and s quarks, may be the ground state of strongly interacting matter (see [29] and references therein). If such a conjecture is true, then there is a possibility of the existence of self-bound pure strange stars as well. In fact, the conversion of NS to strange star may really be a two step process [30]. The first process involves the deconfinement of nuclear to two-flavor quark matter; the second process deals with the conversion of excess down quarks to strange

quarks resulting into a  $\beta$ -equilibrated charge neutral strange quark matter. There are several mechanisms by which the conversion of strange quark may be triggered at the center of the star [31, 32]. The dominant reaction mechanism by which the strange quark production in quark matter occurs is the non-leptonic weak interaction process [33]

$$u_1 + d \leftrightarrow u_2 + s \quad (1)$$

Initially when the quark matter is formed,  $\mu_d > \mu_s$ , and the above reaction converts excess d quarks to s quarks. But in order to produce chemical equilibrium the semileptonic interactions,

$$d(s) \rightarrow u + e^- + \bar{\nu}_e \quad (2)$$

$$u + e^- \rightarrow d(s) + \nu_e \quad (3)$$

play important role along with the above non-leptonic interactions. These imply the  $\beta$ -equilibrium condition  $\mu_d = \mu_u + \mu_e + \mu_{\bar{\nu}}$ ; and  $\mu_s = \mu_d$ .

Actually, the only conserved charges in the system are the baryon number  $n_B$  and the electric charge  $n_Q$ . Since we are assuming neutrinos to leave the system, lepton number is not conserved [10]. Strange chemical potential  $\mu_S$  is zero because strangeness is not conserved. So two of the four chemical potentials ( $\mu_u$ ,  $\mu_d$ ,  $\mu_s$  and  $\mu_e$ ) are independent. In terms of the baryon chemical potential ( $\mu_B$ ), which is equivalent to the quark chemical potential ( $\mu_q = \mu_B/3$ ), and the charge chemical potential ( $\mu_Q$ ) these can be expressed as,  $\mu_u = \mu_q + \frac{2}{3}\mu_Q$ ;  $\mu_d = \mu_q - \frac{1}{3}\mu_Q$ ;  $\mu_s = \mu_q - \frac{1}{3}\mu_Q$ ;  $\mu_e = -\mu_Q$ . These conditions are put as constraints in the description of the thermodynamics of a given system through the PNJL model.

The thermodynamic potential of 2+1 flavor PNJL model for non-zero quark chemical potential is [17]

$$\begin{aligned} \Omega = & \mathcal{U}'[\Phi, \bar{\Phi}, T] + 2g_S \sum_{f=u,d,s} \sigma_f^2 - \frac{g_D}{2} \sigma_u \sigma_d \sigma_s - 6 \sum_{f=u,d,s} \int_0^\Lambda \frac{d^3 p}{(2\pi)^3} E_f \Theta(\Lambda - |\vec{p}|) \\ & - 2T \sum_{f=u,d,s} \int_0^\infty \frac{d^3 p}{(2\pi)^3} \ln \left[ 1 + 3(\Phi + \bar{\Phi} e^{-\frac{(E_f - \mu_f)}{T}}) e^{-\frac{(E_f - \mu_f)}{T}} + e^{-3\frac{(E_f - \mu_f)}{T}} \right] \\ & - 2T \sum_{f=u,d,s} \int_0^\infty \frac{d^3 p}{(2\pi)^3} \ln \left[ 1 + 3(\bar{\Phi} + \Phi e^{-\frac{(E_f + \mu_f)}{T}}) e^{-\frac{(E_f + \mu_f)}{T}} + e^{-3\frac{(E_f + \mu_f)}{T}} \right] \end{aligned} \quad (4)$$

where,  $\sigma_f = \langle \bar{\psi}_f \psi_f \rangle$  and  $E_f = \sqrt{p^2 + M_f^2}$  with,  $M_f = m_f - 2g_S \sigma_f + \frac{g_D}{2} \sigma_{f+1} \sigma_{f+2}$ .

The effective potential  $\mathcal{U}'(\Phi, \bar{\Phi}, T)$  is expressed in terms of the traced Polyakov loop  $\Phi = (\text{Tr}_c L)/N_c$  and its (charge) conjugate  $\bar{\Phi} = (\text{Tr}_c L^\dagger)/N_c$ , where  $L$  is a matrix in color space given by,  $L(\vec{x}) = \mathcal{P} \exp \left[ -i \int_0^\beta d\tau A_4(\vec{x}, \tau) \right]$ , where  $\beta = 1/T$  is the inverse temperature and  $A_4 = A_4^a \lambda_a$ ,  $A_4^a$  being the temporal component of the Euclidian gluon field and  $\lambda_a$  are the Gell-Mann matrices with adjoint color indices  $a = 1, \dots, 8$ . Assuming a constant  $A_4^a$  and the  $A_i$ 's to be zero for  $(i = 1, 2, 3)$ ,  $\Phi$  and its conjugate  $\bar{\Phi}$ , are treated as classical field variables in PNJL model. The temperature dependent effective potential  $\mathcal{U}'(\Phi, \bar{\Phi}, T)$  is so chosen to have exact  $Z(3)$  center symmetry and is given by,

$$\frac{\mathcal{U}'(\Phi, \bar{\Phi})}{T^4} = \frac{\mathcal{U}(\Phi, \bar{\Phi})}{T^4} - \kappa \ln[J(\Phi, \bar{\Phi})], \quad (5)$$

where,

$$\frac{\mathcal{U}(\Phi, \bar{\Phi}, T)}{T^4} = -\frac{b_2(T)}{2} \bar{\Phi} \Phi - \frac{b_3}{6} (\Phi^3 + \bar{\Phi}^3) + \frac{b_4}{4} (\bar{\Phi} \Phi)^2 \quad (6)$$

with  $b_2(T) = a_0 + a_1 \left(\frac{T_0}{T}\right) + a_2 \left(\frac{T_0}{T}\right)^2 + a_3 \left(\frac{T_0}{T}\right)^3$ , and  $J[\Phi, \bar{\Phi}] = (27/24\pi^2)(1 - 6\bar{\Phi}\Phi + 4(\bar{\Phi}^3 + \Phi^3) - 3(\bar{\Phi}\Phi)^2)$  is the Vandermonde determinant. A fit of the coefficients  $a_i$ ,  $b_i$  is performed to reproduce the pure-gauge Lattice data and  $T_0 = 270$  MeV is adopted in our work. Finally  $\kappa = 0.2$  is used which gives reasonable values for pressure for the temperature range used here at zero baryon density as compared to full Lattice QCD computations.

For simplicity, electrons are considered as free non-interacting fermions [10] and the corresponding thermodynamic potential is,

$$\Omega_e = -\left(\frac{\mu_e^4}{12\pi^2} + \frac{\mu_e^2 T^2}{6} + \frac{7\pi^2 T^4}{180}\right) \quad (7)$$

where,  $\mu_e$  is the electron chemical potential.

### III. RESULTS AND DISCUSSIONS

The thermodynamic potential  $\Omega$  is extremised with respect to the scalar fields under the condition  $\mu_d = \mu_u + \mu_e$  and  $\mu_s = \mu_d$ . The equations of motions for the mean fields  $\sigma_u$ ,  $\sigma_d$ ,  $\sigma_s$ ,  $\Phi$  and  $\bar{\Phi}$  for any given values of temperature  $T$ , quark chemical potential  $\mu_q$  and electron chemical potential  $\mu_e$  are determined through the coupled equations,

$$\frac{\partial \Omega}{\partial \sigma_u} = 0, \quad \frac{\partial \Omega}{\partial \sigma_d} = 0, \quad \frac{\partial \Omega}{\partial \sigma_s} = 0, \quad \frac{\partial \Omega}{\partial \Phi} = 0, \quad \frac{\partial \Omega}{\partial \bar{\Phi}} = 0. \quad (8)$$

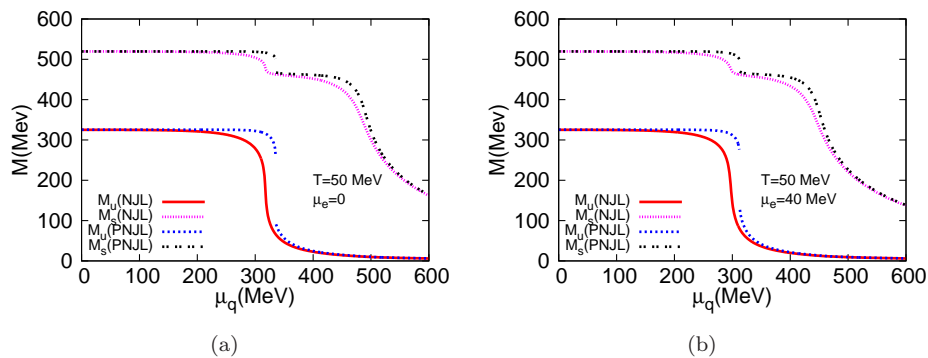


FIG. 1: Constituent quark masses as functions of  $\mu_q$  for (a)  $\mu_e = 0$  MeV and (b)  $\mu_e = 40$  MeV, at  $T = 50$  MeV.

In Fig.1, we show the typical variation of constituent quark masses as a function of  $\mu_q$ , for two representative values of electron chemical potential  $\mu_e = 0$  MeV and  $\mu_e = 40$  MeV, with a fixed temperature  $T = 50$  MeV. At this temperature, both  $m_u$  and  $m_s$  in the PNJL model, show a discontinuous jump at around  $\mu_q = 350$  MeV indicating a first order phase transition. The jump in  $m_s$  is smaller, and is actually a manifestation of chiral transition in the two flavor sector, arising due to the coupling of the strange condensate to the light flavor condensates. On the other hand in the NJL model the quark masses show a smooth variation at this temperature, indicating a crossover. It is important to note that the constituent mass of the strange quark goes down to the current mass at a larger  $\mu_q$  in both the models, leading to sort of a second crossover at around  $\mu_q = 500$  MeV. This will have important implications for some of the thermodynamic observables as we discuss below.

The phase diagrams for NJL and PNJL models are obtained from the behavior of the mean fields, and are shown in Fig. 2(a) and Fig. 2(b) for  $\mu_e = 0$  MeV and  $\mu_e = 40$  MeV respectively. As is evident from the figures, the broad features of the phase diagrams remain same in all cases. The difference between the NJL and PNJL models arise mainly due to the Polyakov loop, whose presence is primarily responsible for raising the transition/crossover temperature in the PNJL model. Thus the CEP for PNJL model occurs at slightly higher  $T$  and lower  $\mu_q$  compared to NJL model. Note that the phase diagram with  $\mu_e = 0$  MeV is identical to the case without  $\beta$ -equilibrium [17]. This is because the minimization conditions (8) are independent of the electrons except through the  $\beta$ -equilibrium conditions. However this is true only so far as the phase diagram is concerned. Various other physical quantities are found to differ even for  $\mu_e = 0$  as discussed below. For non-zero  $\mu_e$  we find a slight lowering of the temperature for the CEP by about 10 MeV. This is an important quantitative difference between the physics of neutron stars and that of compressed baryonic matter created in the laboratory. It is worth to mention that the CEP we have obtained corresponds to chiral phase transition. Generally in standard QCD phase diagram chiral and deconfinement phase transition are shown by a single boundary. However it was argued and elucidated that the two transition lines in  $T - \mu_B$  plane are distinct [34, 35]. In this context we would like to mention that in [36] QCD phase diagram has been studied both for isospin asymmetric and symmetric situations, although they have not considered the  $\beta$ - equilibrium

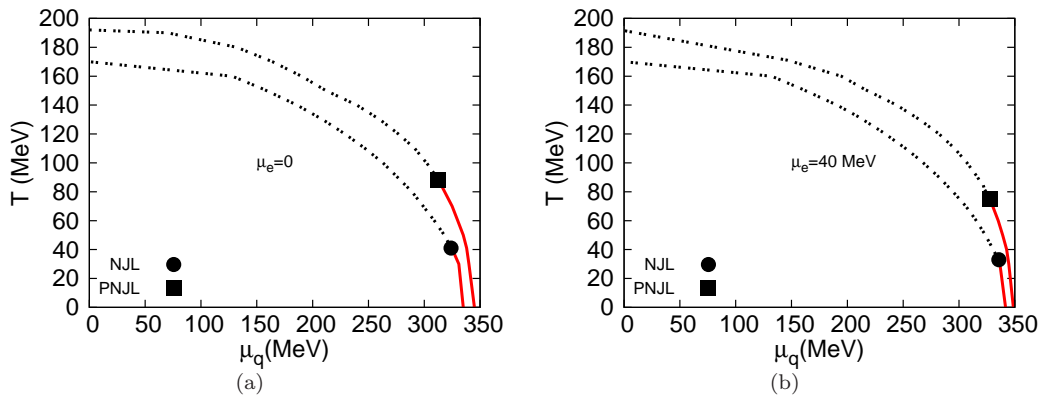


FIG. 2: Comparison of phase diagram in NJL and PNJL model at  $\beta$ -equilibrium for (a)  $\mu_e=0$  ; (b)  $\mu_e=40$ . The solid circle and square represent the CEP for NJL and PNJL model respectively.

scenario. The authors used a two equation of state model, non-linear Walecka model to describe hadronic sector and (P)NJL model for quark sector. It has been shown in [36] that CEP remain unaffected by the isospin asymmetry and the authors found it to be quite generic for a two EOS model.

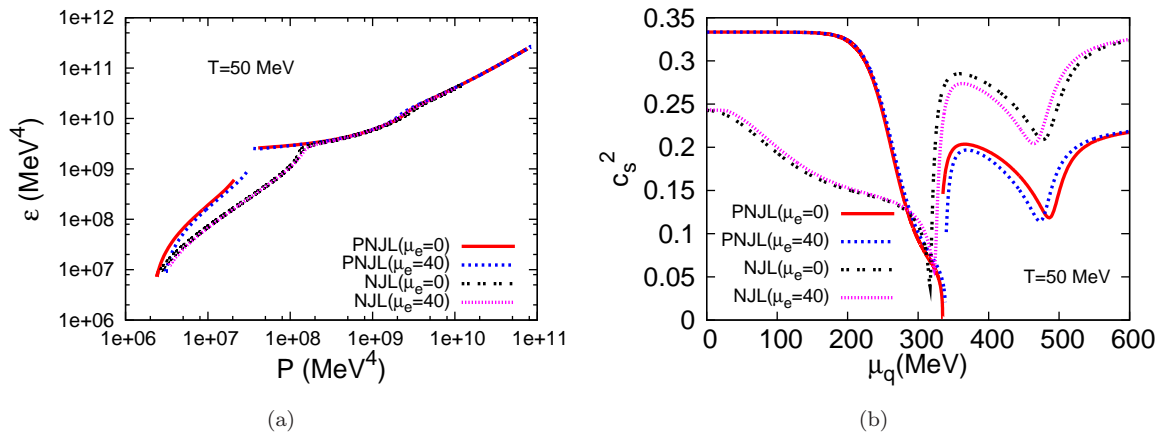


FIG. 3: (a) Equation of state and (b) isentropic speed of sound, for NJL and PNJL models at  $T = 50$  MeV.

The system under investigation can be characterized primarily by the behavior of the EOS. Generally for a many body system, increase in pressure at large densities is indicative of a repulsive behavior of the interaction at large densities (large  $\mu_q$ ) or short distances and an attractive nature at larger distances or lower densities [37, 38]. Consequentially the energy density will show similar behavior. The resulting EOS given by the variation of pressure  $P$  with energy density  $\epsilon$ , is shown in Fig. 3(a) at  $T = 50$  MeV, for both NJL and PNJL models, for the two representative electron chemical potentials. Here again for the PNJL model there exists a discontinuity due to a first order nature of the transition, whereas for NJL model the EOS is smooth. Beyond this region a smaller steepening in  $\epsilon$  is visible, that occurs due to second crossover feature noted above as the strange quark condensate starts to melt. A possible implication for this small surge may be that in a strange quark star, at a given central density, the pressure would be somewhat lesser than the situation without this surge.

Generally, the EOS can be used to study the dynamics of neutron star and that of heavy-ion collisions through the respective flow equations. The main differences would be due to the presence of  $\beta$ -equilibrium and the back reaction of the non-trivial space-time metric on the EOS for neutron stars. Such a comprehensive comparative study will be taken up in a later work.

In Fig. 3(b), the variation of the isentropic speed of sound squared  $c_s^2 = \partial P / \partial \epsilon$  is plotted against  $\mu_q$  at  $T = 50$  MeV. In the NJL model the  $c_s^2$  starts from a non-zero value, steadily decreases and then shows a sharp fall around the crossover region at  $\mu_q \sim 320$  MeV. This is followed by a sharp rise, a dip and then approaches the ideal gas value of  $1/3$ . In contrast the  $c_s^2$  in the PNJL model starting from the ideal gas value remains almost constant up to  $\mu_q \sim 200$  MeV and then falls sharply to almost zero. This is followed by a discontinuous jump, a similar dip at  $\mu_q \sim 500$  MeV

and a gradual approach to a non-zero value quite different from the ideal gas limit.

The difference at  $\mu_q = 0$  MeV occurs specifically due to the Polyakov loop which suppresses any quark-like quasi-particles. As a result the  $c_s^2$  is completely determined by the ideal electron gas. On the other hand those quasi-particles with heavy constituent masses tend to lower the  $c_s^2$  in the NJL model. The difference at the transition region is again mainly due to the discontinuous phase transition in PNJL model which leads to  $c_s^2$  almost going down to zero, and a crossover in the NJL model where  $c_s^2$  is small but non-zero. In [39] it was noted that for two conserved charges, pressure is not constant any more in the mixed phase, rather its variation becomes slower, resulting in a smaller but non-zero speed of sound. In our computation though we do not find  $c_s^2$  exactly equal to zero, but to confirm such an effect we need a full space-time simulation of the mixed phase through the process of bubble nucleation which is beyond the scope of the present work.

In both the models the dip around  $\mu_q = 500$  MeV arises due to the behavior of the strange quark condensate as discussed earlier. If it were possible to achieve such extremely high densities in heavy-ion experiments, then such a dip would slow down the flow and would result in a larger fire ball life time. At even higher  $\mu_q$  the  $c_s^2$  in NJL model approaches the free field limit quite fast but in the PNJL model it still remains quite low due to the non-trivial interaction brought in by the Polyakov loop. It would be interesting to study the implication of slow speed of sound inside the core of a neutron star.

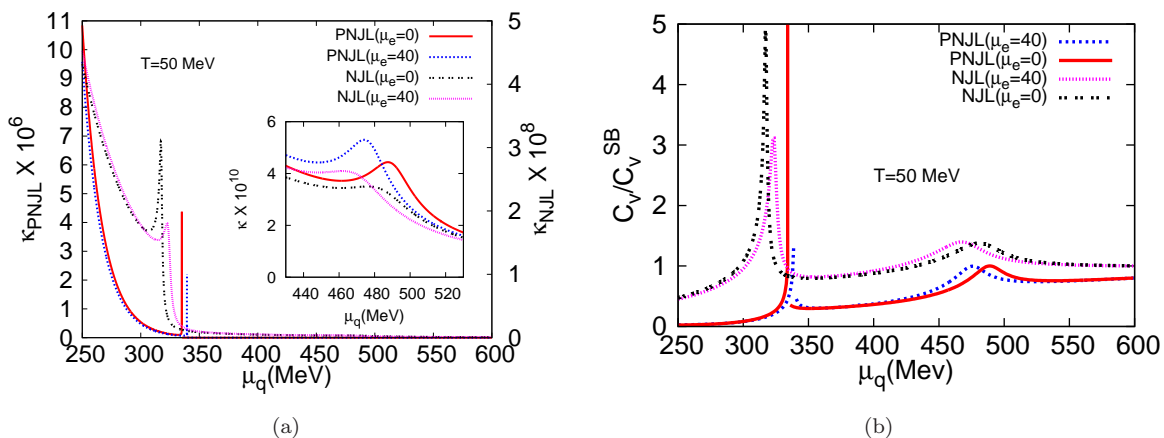


FIG. 4: (a) Variation of compressibility  $\kappa$  with  $\mu_q$ . The peak around  $\mu_q = 500$  MeV is shown in the inset where  $\kappa$  represents the compressibility in both NJL and PNJL models. (b) Variation of specific heat scaled by its Stefan Boltzmann value.

Commensurate with the relative stiffening of the equation of state we find that the compressibility  $\kappa = \frac{1}{n_q^2} \left( \frac{\partial n_q}{\partial \mu_q} \right)_T$ , where  $n_q$  is the quark number density, behaves accordingly. While  $\kappa$  in the NJL model is found to be higher than that of the PNJL model in the hadronic phase, it is just the opposite in the partonic phase as shown in Fig. 4(a). In the NS scenario this would mean that the core of the star would be much softer compared to the crust if described by the PNJL model rather than the NJL model.

The variation of the specific heat  $C_V = T \left( \frac{\partial s}{\partial T} \right)_V$ , where  $s = \left( \frac{\partial P}{\partial T} \right)$  is the entropy density of the system, is shown in Fig. 4(b). For a crossover (here in NJL model) the specific heat shows a peak. For a first order transition (here in the PNJL model) the  $C_V$  is discontinuous. Also we see that the specific heat in the PNJL model is lower than that in the NJL model for a general variation of  $\mu_q$  and  $\mu_e$ . A system described by the PNJL model is thus less susceptible to changing temperature than that described by the NJL model.

The variation of compressibility and specific heat shown here also captures the signature of a phase transition in the PNJL model and a crossover in the NJL model. Both compressibility as well as specific heat are second derivatives of  $\Omega$  and represent respectively the quark number fluctuations and energy fluctuations [37]. Discontinuity in compressibility as well as specific heat indicates a first order phase transition for the PNJL model. At  $\mu_q \sim 500$  MeV, both the models exhibit a small peak due to the onset of melting of the strange quark condensate.

We now consider the net charge density given by  $n_Q = \frac{2}{3}n_u - \frac{1}{3}n_d - \frac{1}{3}n_s - n_e$ , where the number density of individual quarks and electrons are obtained from the relations,  $n_u = \frac{\partial \Omega}{\partial \mu_u}$ ,  $n_d = \frac{\partial \Omega}{\partial \mu_d}$ ,  $n_s = \frac{\partial \Omega}{\partial \mu_s}$ , and  $n_e = \frac{\partial \Omega}{\partial \mu_e}$ . For  $\mu_e = 0$ ,  $n_e = 0$  and we have  $n_u = n_d$ . At large  $\mu_q$ , the number density  $n_s$  of strange quarks become almost equal to the light quark number densities as the constituent masses of strange quarks are reduced significantly. So the net charge density  $n_Q$  will be close to zero and the system will become charge neutral asymptotically as shown in Fig. 5(a). At small  $\mu_q$ ,  $n_Q \ll 1$  as the individual number densities themselves are exceedingly small. In fact this feature continues till

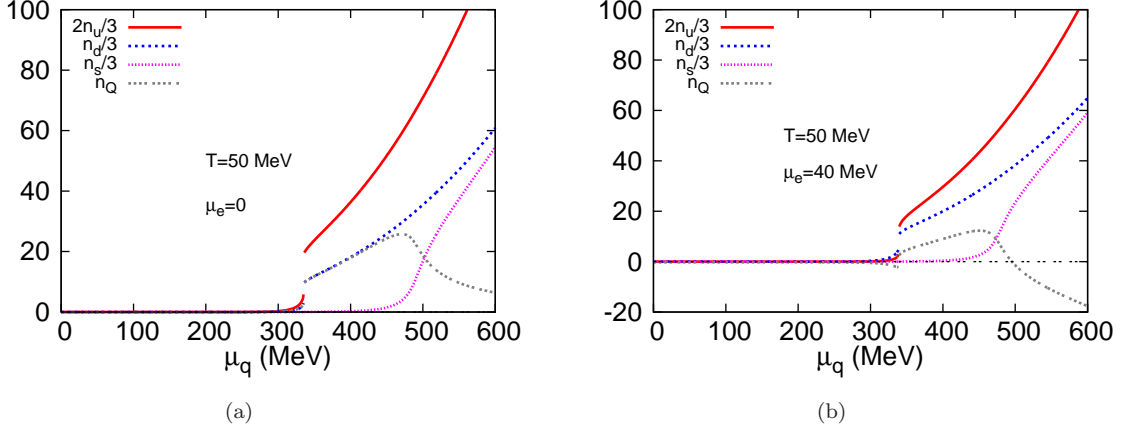


FIG. 5: Total charge and quark number densities scaled by  $T^3$  as a function of quark chemical potential in the PNJL model

the transition region where the light constituent quark masses drop sharply giving rise to non-zero number densities. Therefore  $n_Q$  shows a non-monotonic behavior, rising from almost zero it reaches a maxima at certain  $\mu_q$  determined mainly by the melting of the strange quark condensate and thereafter decreases steadily towards zero.

For higher  $\mu_e$ , charge neutral configuration is possible even at non-zero moderate values of  $\mu_q$ . For small  $\mu_q$ , it is the  $n_e$  which dominates and keeps  $n_Q$  negative. As soon as  $n_u$  becomes large with increasing  $\mu_q$ ,  $n_Q$  goes through zero and becomes positive. Now since  $\mu_s$  and  $\mu_d$  are greater than  $\mu_u$  due to  $\beta$ -equilibrium, both  $n_s$  and  $n_d$  start to grow faster with the increase of  $\mu_q$ . Finally at some  $\mu_q$  the net charge becomes zero due to the mutual cancellation of  $n_u$ ,  $n_d$ , and  $n_s$ , and thereafter it remains negative for higher  $\mu_q$  as  $d$  and  $s$  quarks overwhelms the positively charged  $u$  quark. The electron number density is fixed for a fixed value of  $\mu_e$  and  $T$ , and it is negligible compared to the quark number densities at high  $\mu_q$ . The behavior of  $n_Q$  is similar for both PNJL and NJL model though the actual values of the various chemical potentials for the charge neutrality conditions vary.

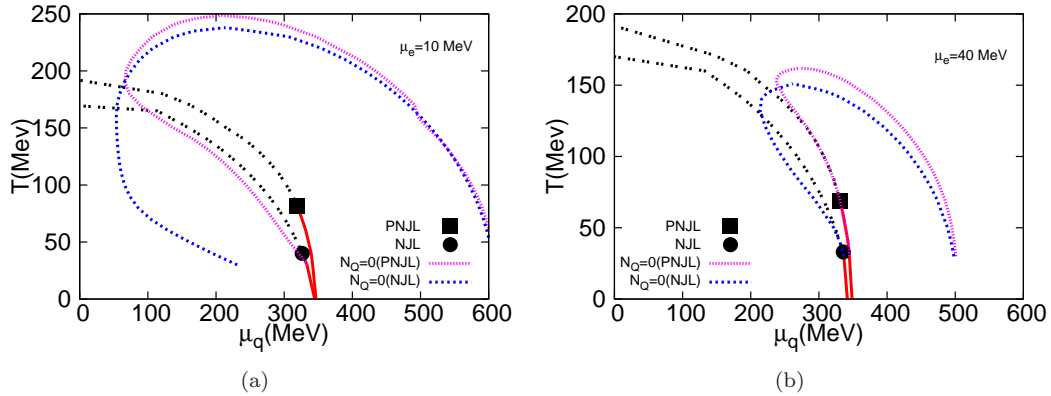


FIG. 6: Comparison of charge neutral trajectory in NJL and PNJL model at (a)  $\mu_e=10$  ; (b)  $\mu_e=40$

Given that one may be interested in the charge neutral condition *e.g.* in the case of neutron stars, in Fig. 6 the charge neutral trajectories for NJL model are compared with those of PNJL model along with the phase diagrams. The trajectories are quite interesting in that they are closed ones pinned on to the  $\mu_q$  axis. They start off close to  $\mu_q = M_{vac}$ , the constituent quark mass in the model in vacuum. They make an excursion in the  $T - \mu_q$  plane and join back at a higher  $\mu_q$ . There is a maximum temperature  $T_Q$  up to which the trajectory goes. Beyond this temperature no charge neutrality is possible. Below this temperature we have essentially two values of  $\mu_q$  where charge neutrality occurs. There are significant differences between the contours of NJL and PNJL model in the hadronic phase. However beyond the transition and inside the deconfined region, the differences subside as the Polyakov loop relaxes the confining effect leading to the PNJL model behaving in a similar way to that of the NJL model.

The behavior of the charge neutral contour is highly dependent on  $\mu_e$ . With increasing  $\mu_e$  the contour gradually closes in towards the transition line. For a given  $T$  there are two  $\mu_q$  values where charge neutrality is obtained – one on the hadronic side and one on the partonic side. As a result of the closing in of the contour, these two values

come closer to the transition line from opposite sides with increasing  $\mu_e$ . Higher the  $\mu_e$  closer we are to the transition region. Now suppose we are looking for an isothermal evolution of a system, or the isothermal configuration of a system such as the NS. Given the constraint of charge neutrality we would have a varying  $\mu_e$  as the density profile changes. Similarly if  $\mu_e$  is held constant then charge neutrality would not allow the temperature to remain fixed throughout and the evolution would take place along the contours described above. So in general a combination of  $T$  and  $\mu_e$  is expected to maintain charge neutrality in a given system. A practical picture of NS which has a profile of low density crust to gradual increase in density to have a highly condensed core would be that there is a complex profile for temperature and  $\mu_e$  inside the NS. In fact if there exist a hadron-parton boundary, it may be either with high temperature or high electron density.

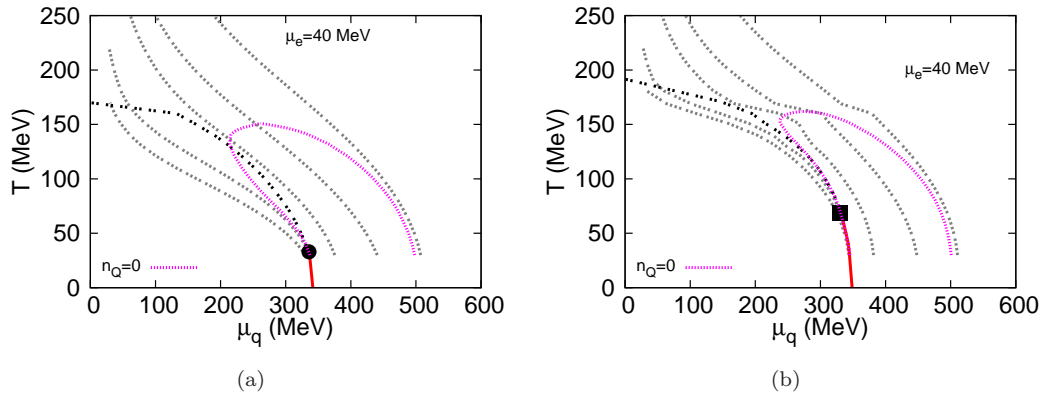


FIG. 7: The contour of scaled baryon number density  $n_B/n_0$ ; (scaled by normal nuclear matter density) along with phase diagram at  $\mu_e=40$  for (a) NJL model and (b) for PNJL model; (From left  $n_B/n_0 = 0.5, 1, 3, 5, 10$  respectively)

To contemplate this scenario in the light of the baryon densities achieved we plot the contours for constant baryon densities, scaled by the normal nuclear matter density ( $n_0 = 0.15 fm^{-3}$ ) in Fig. 7 for  $\mu_e = 40$  MeV. The charge neutral trajectories are also plotted along with the phase boundary. Obviously with increasing baryon (quark) chemical potential baryon density would increase. What is interesting is the fact that high densities can also occur for lower chemical potential if the temperature is higher. For both NJL and PNJL model at and above 3 times nuclear matter density the matter seems to be always in the partonic phase. A little below this density matter may be in partonic phase if it is at high temperature otherwise in the hadronic phase at low temperature. Thus the actual trajectory on the phase diagram would determine whether a hadron-parton boundary in the NS is in the mixed phase or in a state of crossover. Within the range of the charge neutral contour we find the baryon density increasing from a very small value to almost 10 times the normal nuclear matter density. If  $\mu_e$  is increased further the baryon densities would also be much higher for a given  $\mu_q$ . So if we assume local charge neutrality as well as isothermal profile along a hadron-parton phase boundary, the baryon density close to the phase boundary may be too large. On the other hand for reasonable densities close to the phase boundary it would be impossible to maintain local charge neutrality along an isothermal curve. In that case it may be possible that the charge neutrality condition takes the system around the CEP to hold on to a reasonable density in the phase boundary region. This leads us to speculate that the transition in a NS itself may also be a cross-over, quite unlike the picture in most of the studies of NS.

The net strangeness fraction ( $n_s/n_B$ ) along with  $n_B/n_0$  is shown in Fig. 8. For a given temperature, there is a critical  $\mu_q$  below which there is no net strangeness formation. At the critical  $\mu_q$  a non-zero  $n_s/n_B$  occurs depending on the  $T$ . This strangeness fraction continues to appear at lower  $T$  for some higher  $\mu_q$ . So a given strangeness fraction can occur only upto a certain critical temperature. The intersection of lines of constant baryon density and strangeness fraction indicates the possibility of evolution of a system to higher (lower) strangeness fraction with increase (decrease) of  $T$  at a constant density. In the range of 5 - 10 times nuclear matter density we see that the strangeness fraction is increasing significantly towards unity indicating a possibility of formation of quark matter with almost equal number of u, d and s quarks. Similar results have also been found in other model studies [8]. Chunks of matter with  $n_s/n_B = 1$ , called strangelets is expected to be stable (metastable up to weak decay) relative to nuclear matter in vacuum [40]. Investigation of these and various other properties of strange matter would be undertaken in future.

Usually the hydrodynamic evolution of a system is expected to follow certain adiabat along which the entropy per baryon number ( $s/n_B$ ) is a constant quantity. Among the various adiabats the system would choose one given its initial conditions. In the context of NS, a fixed entropy per baryon is expected in a proto-neutron star as well which is very different from a cold neutron star. It is usually hot and rich in leptons *i.e.* electrons and trapped neutrinos.



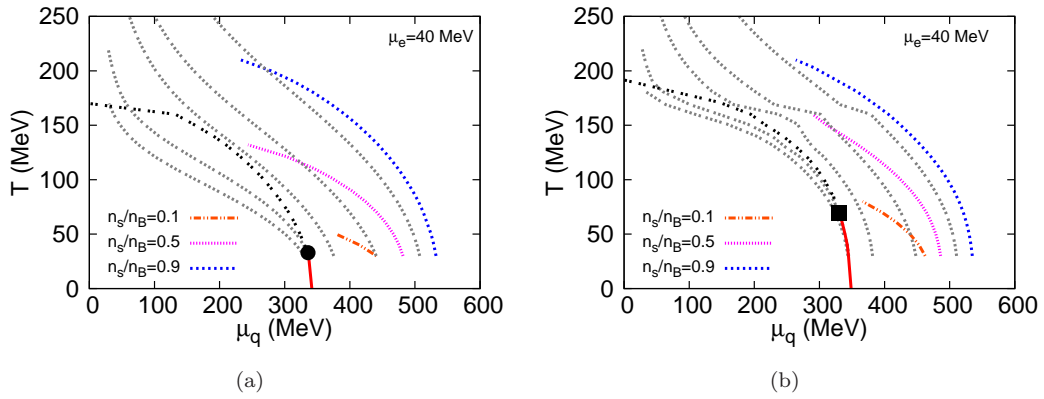


FIG. 8: The contour of net strangeness fraction ( $n_s/n_B$ ) along with  $n_B/n_0$  at  $\mu_e=40$  for (a) NJL model and (b) PNJL model; the values of  $n_B/n_0$  are 0.5, 1, 3, 5 and 10 (from left).

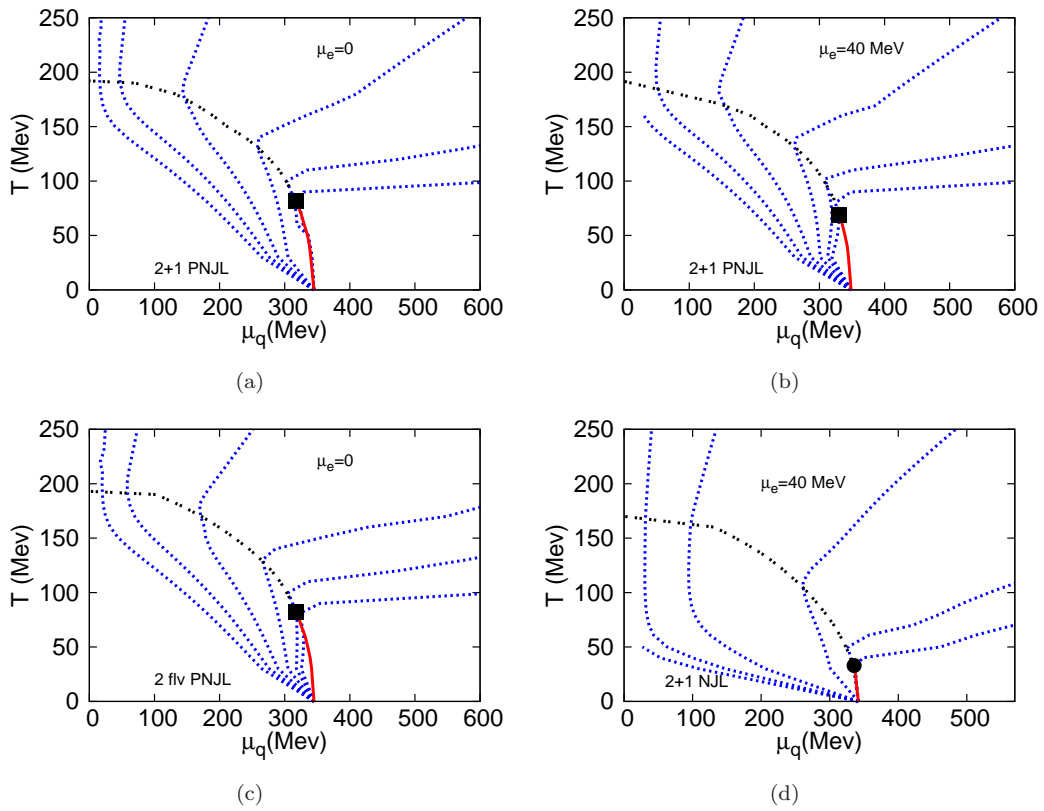


FIG. 9: The isentropic trajectories along with phase diagram for (a) at  $\mu_e=0$ , 2+1-flavor PNJL, (b) at  $\mu_e=40$ , 2+1-flavor PNJL, (c) at  $\mu_e=0$ , 2-flavor PNJL and (d) at  $\mu_e=40$ , 2+1-flavor NJL model.  $s/n_B=300,100,30,10,5,3.5$  (from left).

Few seconds after birth, the matter in the core of a hot NS has almost constant lepton fraction (0.3 -0.4) and entropy per baryon (1 - 2, in units of Boltzmann constant) [41, 42]. The question as to whether the later evolution of the NS can be described to be one close to an adiabat is a matter of debate. On the other hand the commonly used approach of an isothermal evolution looks not quite favorable according to the above discussion on charge neutrality condition.

The behavior of  $s/n_B$  in a plasma and in a hadron gas was analyzed within the framework of an extended Bag model by [43]. A case study of such adiabats was done in NJL model in [44]. It was found that unlike the prescription of adiabats meeting at the CEP given by [45], they meet close to the critical value of  $\mu_q$  at  $T = 0$  which is incidentally equal to the constituent quark mass  $M_{vac}$  in the model in vacuum. It was argued in [44] that as  $T \rightarrow 0$ ,  $s \rightarrow 0$  by the third law of thermodynamics. Hence in order to keep  $s/n_B$  constant,  $n_B$  should go to zero. This condition is

satisfied when  $\mu_q = M_{vac}$  of the theory. These authors also found similar results for the linear sigma model. In the PNJL model the introduction of Polyakov loop produced a slight change in the configuration of the adiabats [46]. The constraint on the strangeness number to be zero also was found not to have a very significant effect [47].

The corresponding picture of isentropic trajectories with the condition of  $\beta$ -equilibrium is shown in Fig. 9. Four cases are depicted here. Fig. 9(a) and Fig. 9(b) show the cases with 2+1 PNJL model at  $\mu_e = 0$  MeV and  $\mu_e = 40$  MeV respectively. From these two figures we find that the electron density does not have a significant effect on the isentropic trajectories. This means that the quark degrees of freedom seem to have dominant effect in entropy over the electrons. The case with  $n_s = 0$ , *i.e.* effectively for a 2-flavor system is shown in Fig. 9(c). In general the situation is similar. For small  $\mu_q$  there is almost no change in Fig. 9(c) and Fig. 9(a) as both the cases are identical to 2 flavors. At intermediate values strange quarks start to pop out. Now the contours in Fig. 9(c) appear to be shifted and bent towards higher  $\mu_q$ . This is because for 2 flavors, a given baryon number density appears at a higher  $\mu_q$  than that for 2+1 flavors. Hence to get a fixed  $s/n_B$  the  $\mu_q$  required is also higher. At even higher  $\mu_q$  the thermal effects are negligible and hence  $s/n_B$  become almost independent of the degrees of freedom. Thus again the contours become identical.

The results in the NJL model are significantly different from that of the PNJL model as can be seen by comparing the PNJL results with that of the NJL model shown in Fig. 9(d). Even for low  $T$  and  $\mu_q$  there is a significant entropy generation as there is no Polyakov loop to subdue the same. Similar differences continue to appear even in the partonic phase.

Considering a system that has been compressed to a few times the nuclear matter density it can try to relax back to lower densities along the adiabats. Interestingly the isentropic trajectories in the high density domain seem to behave as isothermals in the PNJL model. However as soon as the system converts into the hadronic phase, the adiabats drive it to a steep fall in temperature. We would like to mention that for a hadronic proto neutron star with beta-equilibrated nuclear matter with nucleons and leptons in the stellar core, the EOS evaluated in Bruckner–Bethe–Goldstone theory, was found to be similar for both isothermal and isentropic profiles [48].

In Ref.[49] isentropic trajectories were obtained in PNJL model without the constraint of  $\beta$ -equilibrium, for two different sets of parameters corresponding to an ultraviolet cutoff in the zero temperature integrals only (case I) and the same in all integrals (Case II). Here we considered only the first case for regularisation and find similar results.

While the possibility that a neutron star can be described using adiabatic conditions is a point to be pondered about, we note here that an excursion of the phase diagram of a  $\beta$ -equilibrated matter is highly possible even in heavy-ion collisions to some extent. This is because both the isentropic lines as well as the characteristics of the phase boundary are quite similar for a wide variation of  $\mu_e$  and  $\mu_q$ . At the same time one should remember that in the laboratory conditions  $n_s$  is strictly zero. Anyway if a system is found to have travelled along an adiabat with  $s/n_B \simeq 3$  to 4, it has most probably traversed close to the CEP. One can therefore try to correlate different observables like the enhancement of fluctuations of conserved charges and  $s/n_B$  to be in the above range to study the approach towards the CEP in heavy-ion collisions.

#### IV. SUMMARY AND CONCLUSION

In this paper we have studied the 2+1 flavor strongly interacting matter under the condition of  $\beta$ -equilibrium. We have presented a comparative study of NJL versus PNJL model. The phase diagrams in these two models are broadly similar, but quantitatively somewhat different. The presence of the Polyakov loop delays the transition for larger values of temperature for a given quark chemical potential. As a result the CEP in the PNJL model is almost twice as hot as that in the NJL model. We have illustrated characteristics of the phase diagram with the behavior of some thermodynamic quantities like the constituent mass, compressibility, specific heat, speed of sound and the equation of state for  $\mu_e = 0$  MeV and  $\mu_e = 40$  MeV at  $T=50$  MeV. We found striking differences between the NJL and PNJL model in terms of the softness of the equation of state in the hadronic and partonic phases.

The behavior of electric charge and baryon densities in the two models also differ in the hadronic phases to some extent. The differences become less with increasing electron density. We explained how the charge neutral trajectory is important in deciding the path along which the core of NS can change from hadronic to quark phase. For all values of  $\mu_e$  we find that the contours are all closed ones and give a restricted range of temperature and densities that are allowed. We speculated a possible scenario in which the quark-hadron transition in a NS would be a crossover. Again the baryon density contours seemed to suggest that if a system has baryon density three times the nuclear matter density it is quite surely in the partonic phase. We also found that the strangeness fraction increases steadily with increasing baryon density implying a possibility of having a strange NS.

The isentropic trajectories were obtained along which a system in hydrodynamic equilibrium is expected to evolve. The adiabats flow down from high temperature and low density towards low temperature and  $\mu_q = M_{vac}$ , the constituent quark mass in vacuum. The adiabats then steeply rise along the transition line, thereafter goes towards

higher densities with almost a constant slope. For small  $s/n_B$  ratio the slope is so small that the isentropic trajectories almost become isothermal trajectories as well.

To summarize the scenario inside neutron stars we note that inside a newly born NS the temperature drops very quickly and gives rise to a system of low temperature nucleonic matter which may also be populated by hyperons and strange baryons due to high density near the core. The star is assumed to be  $\beta$ -equilibrated and charge neutral. Now it is possible that due to some reason, *e.g.* sudden spin down, this nucleonic matter will start getting converted to predominantly two flavor quark matter within strong interaction time scale. This transition would start at the center and a conversion front moving outward will convert much of the central region of the star. Along the path of the conversion front, each point inside the star may lie on an isentropic trajectory. Gradually this system of predominantly 2 flavor quark matter will get converted to strange quark matter through weak interactions and finally a  $\beta$ -equilibrated charge neutral strange quark matter will be produced. The strangeness production occurs mainly through non-leptonic decay [33], the system is expected to lie on a constant density line and move towards the point with highest strangeness possible at that density. Finally the semi-leptonic processes will take over and system will then evolve along a  $\beta$ -equilibrated charge neutral contour.

The natural extension of the work is to obtain the detailed evolution of a family of neutron stars starting with different initial conditions and gravity effects incorporated. We hope to report the study in a future publication. It would also be important to consider colored exotic states like diquarks [50] that may arise at high densities.

## V. ACKNOWLEDGEMENT

S.M would like to thank CSIR for financial support. A.B. thanks UGC (DRS & UPE) and DST for support. R.R. thanks DST for support. We would like to thank Anirban Lahiri, Paramita Deb and Sibaji Raha for useful discussion and comments.

- 
- [1] Berndt Müller, The Physics of Quark Gluon Plasma, Lecture Notes in Physics (Springer Publication) **225**, 1 (1985).
  - [2] K. Rajagopal and F. Wilczek, At the frontier of particle physics / Handbook of QCD (World Scientific), **3**, 2061 (2001) (arXiv: hep-ph/0011333).
  - [3] D. Blaschke, J. Berdermann, R. Lastowiecki, Prog. Theor. Phys. Suppl. **186**, 81 (2010).
  - [4] N. K. Glendenning, J. Phys. **G 23**, 2013 (1997).
  - [5] J. Schaffner-Bielich, PoS (CPOD07), 062 (2007) (arXiv:0709.1043).
  - [6] G. F. Burgio, M. Baldo, P. K. Sahu, A. B. Santra and H.-J.Schulze, Phys. Lett. **B526**, 19 (2002); G. F. Burgio, M. Baldo, P. K. Sahu, and H.-J. Schulze, Phys. Rev. **C66**, 025802 (2002).
  - [7] M. Alford, M. Brady, M. Paris and S. Reddy, Astrophys. J. **629** 969 (2005).
  - [8] S. K. Ghosh and P. K. Sahu, Int. J. Mod. Phys. **E 2** 575 (1993).
  - [9] S. K. Ghosh, S. C. Phatak and P. K. Sahu, Z. Phys. **A 352** 457 (1995).
  - [10] M. Buballa, Phys. Rept. **407**, 205 (2005).
  - [11] M. Baldo, M. Buballa, G. F. Burgio, F. Neumann, M. Oertel and H.-J. Schulze, Phys. Lett. **B 562**, 153 (2003) and references therein.
  - [12] K. Schertler, S. Leupold and J. Schaffner-Bielich, Phys. Rev. **C 60**, 025801 (1999).
  - [13] M. Baldo, G. F. Burgio, P. Castorina, S. Plumari, D. Zappala, Phys. Rev. **C 75**, 035804 (2007).
  - [14] C. Ratti, M. A. Thaler and W. Weise, Phys. Rev. **D 73**, 014019 (2006).
  - [15] S. K. Ghosh, T. K. Mukherjee, M. G. Mustafa and R. Ray Phys. Rev. **D 73**, 114007 (2006).
  - [16] S. Mukherjee, M. G. Mustafa and R. Ray, Phys. Rev. **D 75**, 094015 (2007); S. K. Ghosh, T. K. Mukherjee, M. G. Mustafa and R. Ray, Phys. Rev. **D 77**, 094024 (2008).
  - [17] A. Bhattacharyya, P. Deb, S. K. Ghosh and R. Ray, Phys. Rev. **D 82**, 014021 (2010).
  - [18] A. Bhattacharyya, P. Deb, A. Lahiri and R. Ray, Phys. Rev. **D 82**, 114028 (2010); *ibid* **D 83**, 014011 (2011).
  - [19] S. B. Ruster, V. Werth, M. Buballa, I. A. Shovkovy and D. H. Rischke, Phys. Rev. **D 72**, 034004 (2005).
  - [20] M. Hanauske, L. M. Satarov, I. N. Mishustin and H. Stöcker, and W. Greiner, Phys. Rev. **D 64**, 043005 (2001).
  - [21] P. Costa, M. C. Ruivo, Yu. L. Kalinovsky and C. A. de Sousa, Phys. Rev. **C 70**, 025204 (2004).
  - [22] P. Costa, M. C. Ruivo and Yu. L. Kalinovsky, Phys. Lett. **B 560**, 171 (2003).
  - [23] J. A. Pons, J. A. Miralles, M. Prakash and J. M. Lattimer, Astrophys. J. **553**, 382 (2001).
  - [24] D. G. Yakovlev and C. J. Pethick, Ann. Rev. Astron. Astrophys. **42**, 169 (2004).
  - [25] D. G. Yakovlev, O. Y. Gnedin, M. E. Gusakov, A. D. Kaminker, K. P. Levenfish and A. Y. Potekhin, Nucl. Phys. **A 752**, 590 (2005) .
  - [26] J. M. Lattimer and M. Prakash, Astrophys. J. **550**, 426 (2001).
  - [27] A. Bhattacharyya, I. N. Mishustin and W. Greiner, J. Phys. **G 37**, 025201 (2010).
  - [28] I. N. Mishustin, M. Hanauske, A. Bhattacharyya, L. M. Satarov, H. Stoecker and W. Greiner, Phys. Lett. **B 552**, 1 (2003).

- [29] E. Witten, Phys. Rev. **D 30**, 272 (1984).
- [30] A. Bhattacharyya, S. K. Ghosh, P. Joarder, R. Mallick and S. Raha Phys. Rev. **C 74**, 06580 (2006).
- [31] C. Alcock, E. Farhi and A. Olinto, Astrophys. J. **310**, 261 (1986).
- [32] N. K. Glendenning, S. Pei and F. Weber, Phys. Rev. Lett. **79**, 1603 (1997).
- [33] S.K. Ghosh, S.C. Phatak and P.K. Sahu, Nucl. Phys. **A 596**, 670 (1996).
- [34] L. McLerran, K. Redlich and C. Sasaki, Nucl. Phys. **A 824**, 86 (2009).
- [35] K. Fukushima, Phys. Rev. **D 77**, 114028 (2008).
- [36] G. Y. Shao *et. al*, Phys. Rev. **D 83**, 094033 (2011); *ibid* **D 84**, 034028 (2011).
- [37] M. Iwasaki, Phys. Rev. **D 70**, 114031 (2004).
- [38] S. V. Molodtsov and Z. M. Zinovjev, Europhys. Lett. **93**, 11001 (2011).
- [39] N. K. Glendenning, Phys. Rev. **D 46**, 1274 (1992).
- [40] E. Farhi and R. L. Jaffe, Phys. Rev. **D 30**, 2379 (1984).
- [41] A. Burrows and J. M. Lattimer, Astrophys. J. **307**, 178 (1986).
- [42] D. Gondek, P. Haensel and J. L. Zdunik, ASP conference series **138**, 131 (1998).
- [43] A. Leonidov, K. Redlich, H. Satz, E. Suhonen and G. Weber, Phys. Rev. **D 50**, 4657, (1994).
- [44] O. Scavenius, A. Mocsy, I.N. Mishustin and D.H. Rishke, Phys. Rev. **C 64**, 045202 (2001).
- [45] M. Stephanov, K. Rajagopal, E. Shuryak Phys. Rev. Lett. **81**, 4816 (1998).
- [46] T. Kahara and K. Tuominen, Phys. Rev. **D 78**, 034015 (2008).
- [47] K. Fukushima, Phys. Rev. **D 79**, 074015 (2009).
- [48] G.F. Burgio and H.-J. Schulze, Phys. Atom. Nucl. **72** 1197 (2009).
- [49] P. Costa, H. Hansen, M. C. Ruivo, and C. A. de Sousa, Phys. Rev. **D 81**, 016007 (2010).
- [50] N. Bentz, T. Horikawa, N. Ishii, A.W. Thomas Nucl. Phys. **A 720**, 95 (2003); S. Roessner, C. Ratti and W. Weise, Phys. Rev. **D 75** 034007 (2007).